A&A 490, 179–187 (2008)
DOI: 10.1051/0004-6361:200809675

Astronomy & Astrophysics

Densities and filling factors of the diffuse ionized gas in the Solar neighbourhood

E. M. Berkhuijsen and P. Müller

Max-Planck-Institut für Radioastronomie, Auf dem Hügel 69, 53121 Bonn, Germany
e-mail: [eberkhuijsen;peter]@mpifr-bonn.mpg.de

Received 28 February 2008 / Accepted 13 July 2008

ABSTRACT

Aims. We analyse electron densities and filling factors of the diffuse ionized gas (DIG) in the Solar neighbourhood.
Methods. We have combined dispersion measures and emission measures towards 38 pulsars at distances known to better than 50%, from which we derived the mean density in clouds, N_c, and their volume filling factor, F_v, averaged along the line of sight. The emission measures were corrected for absorption by dust and contributions from beyond the pulsar distance.
Results. The scale height of the electron layer for our sample is 0.93±0.13 kpc and the midplane electron density is 0.023±0.004 cm^{-3}, in agreement with earlier results. The average density along the line of sight is $\langle n_e \rangle = 0.018 \pm 0.002$ cm^{-3} and is nearly constant. Since $\langle n_e \rangle = F_v N_c$, an inverse relationship between F_v and N_c is expected. We find $F_v(N_c) = (0.011 \pm 0.003)\, N_c^{-1.20\pm0.13}$, which holds for the ranges $N_c = 0.05{-}1$ cm^{-3} and $F_v = 0.4{-}0.01$. Near the Galactic plane the dependence of F_v on N_c is significantly stronger than away from the plane. F_v does not systematically change along or perpendicular to the Galactic plane, but the spread about the mean value of 0.08 ± 0.02 is considerable. The total pathlength through the ionized regions increases linearly to about 80 pc towards $|z| = 1$ kpc.
Conclusions. Our study of F_v and N_c of the DIG is the first one based on a sample of pulsars with known distances. We confirm the existence of a tight, nearly inverse correlation between F_v and N_c in the DIG. The exact form of this relation depends on the regions in the Galaxy probed by the pulsar sample. The inverse F_v–N_c relation is consistent with a hierarchical, fractal density distribution in the DIG caused by turbulence. The observed near constancy of $\langle n_e \rangle$ then is a signature of fractal structure in the ionized medium, which is most pronounced outside the thin disk.

Key words. Galaxy: disk – H II regions – ISM: clouds – ISM: structure

1. Introduction

The full-sky Hα maps of the Milky Way that have recently become available (Dickinson et al. 2003; Finkbeiner 2003; Bennett et al. 2003; Hinshaw et al. 2007) show a spectacular variation in intensity and structure. The classical H II regions in the disc are surrounded by extended, diffuse ionized gas (DIG) visible up to high latitudes, and supernova explosions, shocks and turbulence in the interstellar medium (ISM) have produced a wealth of cloud shapes, filaments, shells and voids.

Madsen et al. (2006) found the variations in structure to be accompanied by variations in electron temperature. They derived a mean temprature of the DIG of about 8000 K with strong differences between lines of sight.

A number of authors derived a scale height of the DIG in the Solar neighbourhood of about 1 kpc from the increase of the dispersion measures of pulsars with increasing distance to the Galactic plane (Reynolds 1991b; Bhattacharia & Verbunt 1991; Nordgren et al. 1992; Gomez et al. 2001; Cordes & Lazio 2003). Using dispersion measures towards 4 pulsars in globular clusters, Reynolds (1991a) obtained a filling fraction of the DIG of $\lesssim$0.2 through the full layer and a mean density in clouds of about 0.08 cm^{-3}. This was recently confirmed by Berkhuijsen et al. (2006) from a much larger pulsar sample. These authors also found an increase of the filling factor with distance from the plane. Already the scanty data that were available to Kulkarni & Heiles (1988) had indicated such an increase.

Turbulence causing hierarchical, fractal structure leads to an inverse relationship between the mean filling factor along the line of sight, F_v, and the mean density in ionized regions, N_c (Fleck 1996; Elmegreen 1998, 1999). Pynzar (1993), who was the first to investigate this relationship, derived $F_v \propto N_c^{-0.7}$ for a combination of DIG and H II regions, which was confirmed by Berkhuijsen (1998). In an extensive study, Berkhuijsen et al. (2006, hereafter BMM) obtained $F_v \propto N_c^{-1.07\pm0.03}$ for the DIG from a sample of 157 pulsars at latitudes $|b| > 5°$. They used dispersion measures from the catalogue of Hobbs & Manchester (2003; see also Manchester et al. 2005), emission measures from the WHAM survey (Haffner et al. 2003), corrected for absorption (Diplas & Savage 1994) as well as for contributions from beyond the pulsars, and pulsar distances from the model of the electron distribution in the Galaxy of Cordes & Lazio (2002). The statistical error in pulsar distances <3 kpc, where 75% of the pulsars in the sample are located, is about 25% which is much smaller than the intrinsic spread in the dispersion measures and emission measures. Therefore, random errors in the model distances will not have influenced the statistical results. However, the distances from the model may also contain a systematic error. Based on these distances, the radial distribution of pulsars has a maximum at $R = 3.5$ kpc from the Galactic centre (Lorimer 2004; Yusifov & Küçük 2004), whereas other population I objects (H2, H I, H II regions) peak near $R = 5$ kpc. The smoothness of the electron density model may lead to pulsar distances that are too large.

So it is important to check the results of BMM for pulsars with distances derived from observations. Since BMM did their work, the sample of pulsars with measured distances has increased considerably. Our new analysis is based on 38 pulsars,

the distances of which are known to better than 50%. A further decrease of the constraint on the distance errror would make the sample too small for a statistical analysis. We also used an improved absorption correction of the emission measure towards each pulsar instead of the statistical correction applied by BMM.

2. Basics and data

2.1. Basic relations

The expressions for dispersion measure, DM, and emission measure, EM, towards a pulsar at distance D (in pc) can be written in various ways:

$$DM = \int_0^{\rm D} n_{\rm e}(l){\rm d}l = \langle n_{\rm e}\rangle D = N_{\rm c}F_{\rm v}D = N_{\rm c}L_{\rm e}, \quad (1)$$

$$EM = \int_0^{\rm D} n_{\rm e}^2(l){\rm d}l = \langle n_{\rm e}^2\rangle D = N_{\rm c}^2F_{\rm v}D = N_{\rm c}^2L_{\rm e}, \quad (2)$$

where $n_{\rm e}(l)$ (in cm^{-3}) is the local electron density at point l along the line of sight, $L_{\rm e}$ (in pc) the total pathlength through the regions containing free electrons (clouds, clumps) and $N_{\rm c}$ (in cm^{-3}) the average density in these regions; between clouds the electron density is assumed to be negligible (see Fig. 1 in BMM). Furthermore, $\langle n_{\rm e}\rangle$ and $\langle n_{\rm e}^2\rangle$ are averages along D, and $F_{\rm v} = L_{\rm e}/D$ is the fraction of the line of sight in clouds, which approximates the volume filling factor $F_{\rm v}$ if there are several clouds along the line of sight (BMM). Note that the third equality in Eq. (2) is only valid when the average density of each cloud $n_{\rm c}$ along the line of sight is the same: then $\langle n_{\rm e}^2\rangle = \langle n_{\rm c}^2\rangle F_{\rm v} = N_{\rm c}^2F_{\rm v}$. Thus $N_{\rm c}$ and $F_{\rm v}$ are approximations of the true average density in clouds and their filling factor.

Combining Eqs. (1)[1] and (2) we have

$$N_{\rm c} = EM/DM, \quad (3)$$

$$F_{\rm v} = DM^2/EM\,D. \quad (4)$$

The derived quantities $N_{\rm c}$ and $F_{\rm v}$ are connected by the simple relation $\langle n_{\rm e}\rangle = F_{\rm v}N_{\rm c}$ following from the third equality in Eq. (1). As the mean electron density in clouds will not be constant, our estimate of $N_{\rm c}$ will be too high because of the $n_{\rm e}^2$ dependence of EM. Recently, Hill et al. (2008) found that the ratio between the most probable density and $N_{\rm c}$ varies between 0.95 and 0.4 in the mildly supersonic cases of their MHD simulations (scaled to observations). Thus, our values of $N_{\rm c}$ may be too high by a factor $\lesssim$2; the corresponding values of $F_{\rm v}$ will then be too low by the same factor.

2.2. The data

We collected a sample of 78 pulsars with distances known to better than 50% from the literature. This error is negligible compared to the large intrinsic spread in DM (a factor of 2) and EM (a factor of 4). The sample consists of 52 pulsars from the list of Gomez et al. (2001), where we used more recent distances when available, and 26 pulsars with parallactic distances taken from Hobbs et al. (2005, and references therein).

The dispersion measures came from the catalogue of Manchester et al. (2005). To find the emission measures in the pulsar directions we used the full-sky Hα map of Finkbeiner (2003) corrected for extinction as described by Dickinson et al. (2003), who argued that only one third of the dust in the line of sight effectively absorbs Hα emission. The extinction-corrected emission measure is

$$EM_{\rm c} = EM \times 0.34\,A \quad \text{with } A = \exp\left(2.4\,E(B-V)\right),$$

where EM is the observed emission measure and A the correction recommended by Finkbeiner (2003). Corrections of more than 1 mag are uncertain and cannot be used. Therefore we had to remove 38 pulsars from the sample, most of which are at latitudes $|b| < 5°$. We also removed 2 pulsars with high EM and DM (J0613−0200 and J1807+0943) indicating H II regions on their lines of sight. Thus for the analysis a sample of 38 pulsars is available, for 23 of which a parallactic distance is known. The errors in the distances to 28 pulsars are smaller than 20% ($\Delta D/D < 0.2$) and those in the distances to the other 10 pulsars are less than 50% ($0.2 < \Delta D/D < 0.5$). As 21 pulsars are located at $D < 2$ kpc, the sample is heavily weighted to the Solar neighbourhood; 13 pulsars are in globular clusters at distances >2 kpc. The main parameters of the 38 pulsars in the sample are listed in Table 1, which also gives the references to the distances used. The sightlines to these pulsars probe the DIG.

In the direction of nearby pulsars and of pulsars near the Galactic plane a significant amount of the emission measure originates beyond the pulsar (see Fig. 5 in BMM). Reynolds (1997) and Haffner et al. (2003) have shown that the vertical electron distribution derived from Hα observations is fairly well described by an exponential. Then the emission measure up to the pulsar, $EM_{\rm p}$, is obtained from

$$EM_{\rm p}\sin|b|(z) = EM_{\rm c}\sin|b|\left(1-\exp\left(-|Z_{\rm p}|/h_{\rm e}\right)\right), \quad (5)$$

where $Z_{\rm p}$ is the distance of the pulsar to the Galactic plane and $h_{\rm e}$ is the scale height of $n_{\rm e}^2(z)$. Deviations from a smooth, plane-parallel layer will cause scatter in $EM_{\rm p}$. The mean of $EM_{\rm c}\sin|b|$ for our sample is 2.8 ± 0.3 cm^{-6} pc, which is the extinction-corrected emission measure through the full layer. We derive the scale height $h_{\rm e}$ in the next section.

3. Scale height of electrons

We first estimated the scale height $h_{\rm e}$ of $n_{\rm e}^2(z)$ using Eqs. (12) and (13) of BMM, expecting that also for our sample the average filling factor $F_{\rm v}(z)$ would increase with $|z|$. This yielded 280 pc $< h_{\rm e} <$ 510 pc with a best value of 390 pc, giving the observed maximum values of $DM\sin|b| = 22 \pm 2$ cm^{-3} pc (see Fig. 1) and $EM_{\rm p}\sin|b| = 2.8 \pm 0.3$ cm^{-6} pc. However, for this entire range of $h_{\rm e}$, $F_{\rm v}(z)$ appeared to be essentially constant for our sample (see Fig. 4d), thus also the local filling factor $f(z)$ is $\simeq$const. As is easily seen, this indicates that the scale height of $n_{\rm e}^2(z)$ is about half that of $n_{\rm e}(z)$.

Following BMM, we describe the dispersion measure perpendicular to the Galactic plane as

$$\begin{aligned} DM\sin|b|(z) &= \int_0^{|Z_{\rm p}|} n_{\rm e}(z){\rm d}z = \int_0^{|Z_{\rm p}|} f(z)n_{\rm c}(z){\rm d}z \\ &= f_0 n_{\rm c0} h\left(1-\exp\left(-|Z_{\rm p}|/h\right)\right), \end{aligned} \quad (6)$$

where we assume that $f(z) = f_0$ and the local density in clouds $n_{\rm c}(z)$ is an exponential with midplane value $n_{\rm c0}$ and scale height h; $Z_{\rm p}$ is the distance of the pulsar to the midplane.

[1] Note that we write $F_{\rm v}$ and $N_{\rm c}$ where BMM used $\overline{f}_{\rm v}$ and $\overline{n}_{\rm c}$.

Table 1. Parameters of the 38 pulsars in the final sample.

PULSAR Jname	*LONG* [°]	*LAT* [°]	DM^a [$\mathrm{cm^{-3}\,pc}$]	$D \pm \Delta D^b$ [pc]		REF	EM_c [$\mathrm{cm^{-6}\,pc}$]	EM_p	N_c [$\mathrm{cm^{-3}}$]	F_v
J0437−4715	253.40	−42.00	2.65	159	5	1	1.8	0.4	0.137	0.122
J0814+7429	140.00	31.62	6.12	433	8	5	1.9	0.7	0.116	0.122
J0826+2637	197.00	31.70	19.45	360	80	6	4.8	1.6	0.081	0.665
J0953+0755	228.91	43.70	2.96	262	5	5	3.2	1.0	0.351	0.032
J1136+1551	241.91	69.19	4.86	350	20	5	1.5	0.8	0.155	0.090
J1239+2453	252.45	86.54	9.24	850	60	5	1.1	0.9	0.100	0.108
J1456−6843	313.90	−8.50	8.60	450	60	8	32.4	4.3	0.497	0.038
J1932+1059	47.38	−3.88	3.18	330	10	5	18.5	0.9	0.269	0.036
J2018+2839	68.10	−3.98	14.18	950	90	5	35.0	4.6	0.323	0.046
J2022+2854	68.86	−4.67	24.64	2300	800	5	38.5	12.6	0.513	0.021
J2022+5154	87.86	8.38	22.65	1900	250	5	12.6	5.6	0.247	0.048
J0922+0638	225.42	36.39	27.27	1210	90	7	7.3	5.7	0.209	0.108
J1537+1155	19.85	48.30	11.61	1080	150	1	2.7	2.2	0.192	0.056
J1713+0747	28.75	25.22	15.99	910	80	1	4.9	2.8	0.172	0.102
J1744−1134	14.79	9.18	3.14	470	95	1	21.4	3.2	1.005	0.007
J1909−3744	359.73	−19.60	10.39	1140	50	1	8.1	4.5	0.431	0.021
J0659+1414	201.11	8.26	13.98	290	30	4	14.0	1.2	0.085	0.567
J2145−0750	47.78	−42.08	9.00	500	200	9	1.7	0.9	0.098	0.184
J1022+1001	231.79	51.10	10.25	400	145	1	2.7	1.3	0.129	0.198
J1024−0719	251.70	40.52	6.48	520	270	1	2.3	1.2	0.183	0.068
J2124−3358	10.93	−45.44	4.60	250	165	1	2.8	0.9	0.189	0.098
J0030+0451	113.14	−57.61	4.33	300	90	2	1.0	0.4	0.099	0.146
J1509+5531	91.32	52.29	19.61	2370	220	3	1.0	1.0	0.049	0.169
J0534+2200	184.56	−5.78	56.79	2000	75	11	23.3	8.1	0.143	0.198
J1740−5340c	338.20	−11.90	71.80	2300	20	11	37.8	24.0	0.335	0.093
J0141+6009	129.10	−2.10	34.80	2750	150	11	29.0	5.6	0.161	0.079
J1910−5959c	336.50	−25.60	33.68	4000	250	11	3.2	3.1	0.092	0.091
J1824−2452c	7.80	−5.58	119.86	5700	750	11	76.6	53.1	0.443	0.047
J1701−3006c	353.60	7.30	114.56	6900	900	11	59.4	50.2	0.438	0.038
J1911+0101c	36.11	−3.92	202.68	9500	800	12	39.2	29.3	0.145	0.147
J1823−3021c	2.79	−7.91	86.84	8000	800	11	26.8	24.2	0.279	0.039
J1804−0735c	20.79	6.77	186.32	8400	1900	11	35.5	31.2	0.168	0.132
J1748−2021c	7.73	3.80	220.40	8400	2100	11	88.7	61.6	0.279	0.094
J1721−1936c	4.86	9.74	75.70	8600	1100	11	21.4	20.4	0.270	0.033
J0024−7204c	305.92	−44.89	24.60	4500	250	11	3.6	...	...	...
J1518+0205c	3.8	46.80	29.47	7500	400	11	2.1	...	...	...
J1641+3627c	59.00	40.91	30.36	7700	380	11	1.8	...	...	...
J2129+1210c	65.01	−27.31	67.31	10300	650	11	5.0	...	...	...

[a] Hobbs & Manchester (2003): www.atnf.csiro.au/research/pulsar/psrcat.
[b] Mean of absolute values of positive and negative error.
[c] In globular cluster. The last four pulsars are at $|z| > 3$ kpc, and only used in the determination of the electron scale height (see Fig. 1).
References. (1) Hotan et al. (2006); (2) Lommen et al. (2006); (3) Chatterjee et al. (2005); (4) Brisken et al. (2003); (5) Brisken et al. (2002); (6) Gwinn et al. (1986); (7) Chatterjee et al. (2001); (8) Bailes et al. (1990); (9) Löhmer et al. (2004); (10) Stairs et al. (1998); (11) Gomez et al. (2001); (12) Heitsch & Richtler (1999).

Similarly, the emission measure perpendicular to the Galactic plane is

$$EM_p \sin|b|(z) = \int_0^{|Z_p|} n_e^2(z)\mathrm{d}z = \int_0^{|Z_p|} f(z) n_c^2(z)\mathrm{d}z$$
$$= f_0 n_{c0}^2 h \left(1 - \exp\left(-2|Z_p|/h\right)\right)/2, \quad (7)$$

where the scale height h_e in Eq. (5) is equal[2] to $h/2$.

We can derive the maximum of $DM \sin|b|$ and the scale height h from the distribution of $DM \sin|b|(z)$ of our sample of 38 pulsars shown in Fig. 1. A two-parameter fit yielded $f_0 n_{c0} h = 21.7 \pm 1.5\,\mathrm{cm^{-3}\,pc}$ and $h = 0.93 \pm 0.13$ kpc, giving $n_e(0) = f_0 n_{c0} = 0.023 \pm 0.004\,\mathrm{cm^{-3}}$. As the maximum of $EM_p \sin|b|$ equals $EM_c \sin|b|$, we have $n_e^2(0)h/2 = f_0 n_{c0}^2 h/2 = 2.8 \pm 0.3\,\mathrm{cm^{-6}\,pc}$ (see Sect. 2); hence $n_e^2(0) = 0.0060 \pm 0.0011\,\mathrm{cm^{-6}}$, $n_{c0} = 0.26 \pm 0.03\,\mathrm{cm^{-3}}$ and $f_0 = 0.09 \pm 0.02$.

We then analysed the data in our sample using $h_e = h/2 = 0.47$ kpc in Eq. (5), leaving out 4 pulsars in globular clusters at $|z| > 3$ kpc. As only a small part of their lines of sight passes through the electron layer, the mean electron densities along the line of sight are unrealistically low. Figure 2 shows the distribution of $EM_p \sin|b|(z)$ for all pulsars. The steady increase of $EM_p \sin|b|$ with $|z|$ agrees well with the expected variation (full line), but the scatter is larger than in Fig. 1.

4. Results

In this section we investigate the dependencies of $\langle n_e \rangle$, $\langle n_e^2 \rangle$, N_c and F_v on $|z|$, and the relationship between F_v and N_c. The statistical treatment is the same as used by BMM and we refer to that paper for details. The results are given in Table 2.

[2] Note that BMM defined h as the scale height of $n_e^2(z)$, thus their h equals our $h_e = h/2$.

Table 2. Statistical relationships derived for the sample of 34 pulsars.

X	Y	Fit	a	b	Corr. coeff.	Student t^6
DM	EM_p	bis[1]	$0.13^{+0.04}_{-0.03}$	1.15 ± 0.07	0.90 ± 0.08	11.8
$DM \cos\|b\|$	$EM_p \cos\|b\|$	"	$0.13^{+0.03}_{-0.02}$	1.15 ± 0.05	0.93 ± 0.06	14.7
$DM \sin\|b\|$	$EM_p \sin\|b\|$	"	0.21 ± 0.04	0.98 ± 0.09	0.82 ± 0.10	8.3
D	$\langle n_e \rangle$	lin[2]	0.018 ± 0.002	$-(2 \pm 6)10^{-4}$	0.52 ± 0.15	3.5
$\|z\|$	$\langle n_e \rangle$	exp[3]	0.019 ± 0.002	-3^{+1}_{-3}	0.72 ± 0.12	5.9
$\|z\|$	$\langle n_e^2 \rangle$	"	0.0045 ± 0.0007	$-1.4^{+0.3}_{-0.6}$	0.77 ± 0.11	6.9
$\|z\|$	N_c	"	$0.24^{+0.04}_{-0.03}$	$-2.6^{+1.0}_{-4.1}$	0.76 ± 0.12	6.6
$\|z\|$	F_v	"	$0.077^{+0.020}_{-0.016}$	[+23][5]	0.63 ± 0.14	4.6
$\|z\|$	$L_e \sin\|b\|$	pow[4]	80 ± 20	1.06 ± 0.15	0.83 ± 0.10	8.5
N_c	F_v	"	$0.011^{+0.003}_{-0.002}$	-1.20 ± 0.13	0.88 ± 0.09	10.2
N_c	L_e	"	24^{+20}_{-11}	-0.85 ± 0.35	0.75 ± 0.12	6.5
N_c	$L_e \sin\|b\|$	"	2 ± 1	-1.6 ± 0.3	0.82 ± 0.10	8.0

Units: DM in cm^{-3} pc, EM and EM_p in cm^{-6} pc, $\langle n_e \rangle$ and N_c in cm^{-3}, $\langle n_e^2 \rangle$ in cm^{-6}, $|z|$ in kpc, L_e in pc.
1) Bisector fit to powerlaw $Y = aX^b$ in $\log X - \log Y$ plane.
2) Linear fit; regression line of Y on X, where $Y = a + bX$.
3) Exponential fit; regression line of $\ln Y$ on $|z|$ with slope $1/b$, where b is the scale height H in kpc.
4) Powerlaw fit; regression line of $\log Y$ on $\log X$.
5) Undetermined: errors $>1/b$.
6) Student test: for a sample of 34 pulsars the correlation is significant at the 3σ level if $t > 3.3$.
All fits are ordinary least-squares fits with errors of one standard deviation.

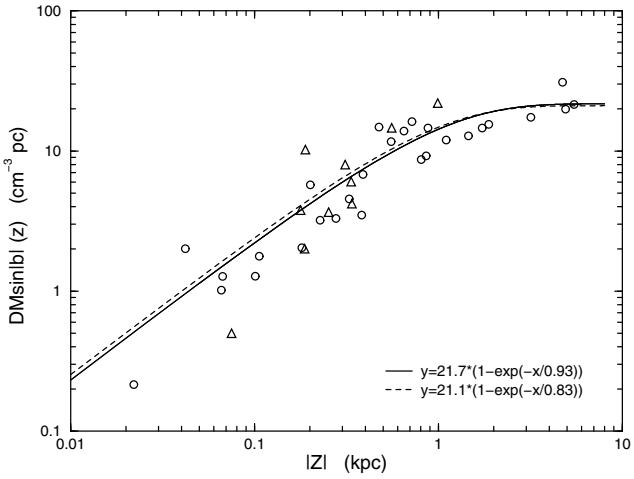

Fig. 1. Dependence of the dispersion measure perpendicular to the Galactic plane, $DM \sin|b|$, on distance to the plane, $|z|$, of the final sample of 38 pulsars. Circles: pulsars with $\Delta D/D < 0.2$; triangles: pulsars with $0.2 < \Delta D/D < 0.5$. Full line: the two-parameter fit to the data; dashed line: fit to the original sample of 78 pulsars, shown for comparison.

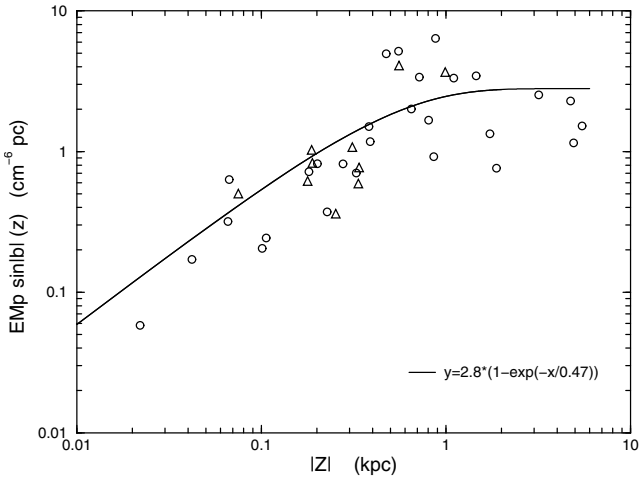

Fig. 2. Dependence of the corrected emission measure perpendicular to the Galactic plane, $EM_p \sin|b|$, on distance to the plane, $|z|$, of the final sample of 38 pulsars. Circles: pulsars with $\Delta D/D < 0.2$; triangles: pulsars with $0.2 < \Delta D/D < 0.5$. Full line: dependence expected for the scale height of 0.47 kpc used in Eq. (5).

We first show in Fig. 3 that EM_p is well correlated with DM: the bisector fit yields $EM_p = (0.13 \pm 0.04) DM^{1.15 \pm 0.07}$ with very high significance. This indicates that both quantities probe the same ionized regions along the line of sight, although the beams used for the Hα observations (up to 1°) also sample regions located around the single sightline to the pulsar. Variations in electron density across the beam will contribute to the scatter in Fig. 3. The components of EM_p and DM along $|z|$ correlate less well than those along the Galactic plane (see Table 2), because of the different scale heights of $n_e^2(z)$ and $n_e(z)$.

4.1. Dependence of $\langle n_e \rangle$, $\langle n_e^2 \rangle$, N_c and F_v on height

Figure 4 presents the various densities and F_v as a function of $|z|$ in the $\log Y - |z|$ plane. Although these variables represent averages along the line of sight, we approximated their $|z|$-distributions by exponentials with scale height H. The fits are listed in Table 2.

The distribution of $\langle n_e \rangle(z)$ in Fig. 4a is effectively constant up to $|z| \simeq 1$ kpc (dashed line), a well known fact first noted by Weisberg et al. (1980). Beyond this height $\langle n_e \rangle$ decreases. A fit to all points (full line) gives a mean value at the midplane of $\langle n_e \rangle_0 = 0.019 \pm 0.02\,cm^{-3}$, in fair agreement with the expected value $\langle n_e \rangle_0 = n_e(0) = 0.023 \pm 0.004\,cm^{-3}$ derived in Sect. 3. The

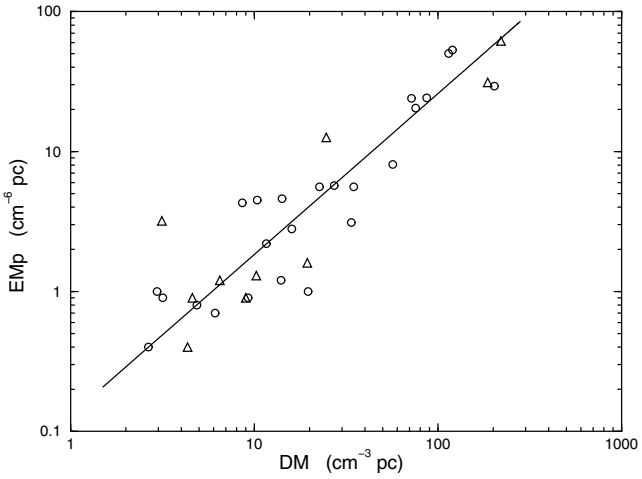

Fig. 3. Comparison of corrected emission measure, EM_p, and observed dispersion measure, DM. Circles: pulsars with $\Delta D/D < 0.2$; triangles: pulsars with $0.2 < \Delta D/D < 0.5$. Full line: bisector fit given in Table 2.

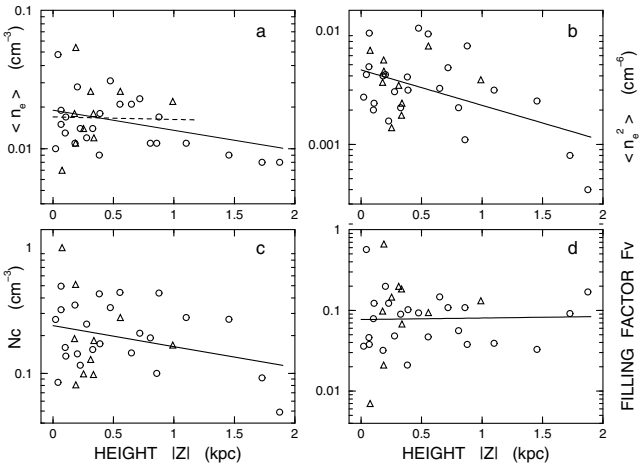

Fig. 4. Electron densities averaged along the line of sight and average volume filling factor as a function of height above the Galactic plane, $|z|$. **a)** Average density $\langle n_e \rangle = DM \sin|b|/|z|$. The dashed line is the exponential fit to the data at $|z| < 1.2$ kpc. **b)** Average of the square of the density $\langle n_e^2 \rangle = EM_p \sin|b|/|z|$. **c)** Mean density in clouds $N_c = EM_p/DM$. **d)** Average volume filling factor $F_v = DM^2/(EM_p D)$. Full lines indicate the exponential fits given in Table 2. Circles: pulsars with $\Delta D/D < 0.2$; triangles: pulsars with $0.2 < \Delta D/D < 0.5$.

scale height is less well determined, though. The spread in the data clearly decreases away from the plane, as was also noted by BMM. This is not due to longer pathlengths, because the spread in the distribution projected along the plane remains constant (not shown). It just shows that the variety in electron density is larger near the Galactic plane than away from the plane.

The other panels in Fig. 4 show the dependencies of $\langle n_e^2 \rangle$, N_c and F_v on $|z|$. All quantities vary considerably about the fitted lines. The mean density in clouds slowly decreases from $0.24\,\mathrm{cm}^{-3}$ at $|z| = 0$ kpc to $0.16\,\mathrm{cm}^{-3}$ at $|z| = 1$ kpc, but at all heights values between $0.08\,\mathrm{cm}^{-3}$ and $0.5\,\mathrm{cm}^{-3}$ occur. The midplane values of the exponential fits in Table 2 agree to within errors with those of $n_e^2(0)$, n_{c0} and f_0 derived in Sect. 3 and the scale height H of $\langle n_e^2 \rangle$ is indeed about half that of $\langle n_e \rangle$ and N_c. This agreement shows that the data are internally consistent.

The slight increase in $F_v(z)$ in Fig. 4d is statisically insignificant, thus $F_v(z)$ is effectively a constant of about 0.08 ± 0.02. This differs from the clear increase in $F_v(z)$ found by BMM for

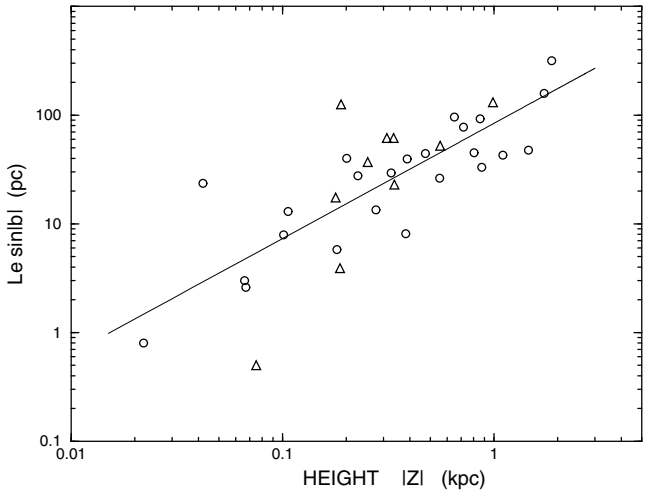

Fig. 5. Dependence of the total pathlength through ionized regions perpendicular to the Galactic plane, $L_e \sin|b|$, on height above the plane. Circles: pulsars with $\Delta D/D < 0.2$; triangles: pulsars with $0.2 < \Delta D/D < 0.5$. Full line: powerlaw fit given in Table 2.

a much larger sample of pulsars. The spread in F_v seems largest near the Galactic plane, but this impression is mainly due to three extreme points of nearby pulsars at low $|z|$: two near $F_v = 0.6$ and one near $F_v = 0.07$. At $|z| > 0.3$ kpc the spread stays within a factor of 4.

If the mean filling fraction remains about constant along the line of sight, the total pathlength through the ionized regions will increase linearly with distance. $L_e \sin|b|(z)$ indeed increases nearly linearly from about 7 pc towards $|z| = 0.1$ kpc to about 80 pc towards $|z| = 1$ kpc (see Fig. 5 and Table 2).

4.2. Dependence of F_v on N_c

One of the indications for turbulence in the ISM is an inverse relationship between filling factor and mean cloud density. This is not only expected on theoretical grounds (Fleck 1996; Elmegreen 1999), but has also been obtained from simulations (Elmegreen 1997; Kowal & Lazarian 2007). Observational evidence, however, is scarce (see Sect. 1).

Since $\langle n_e \rangle$ is about constant (Fig. 4a) and $\langle n_e \rangle = F_v N_c$, we expect an inverse relationship between F_v and N_c. We present this relationship for our sample in Fig. 6. The correlation between F_v and N_c is very good and indeed nearly inverse: the power-law fit yields $F_v(N_c) = (0.011 \pm 0.003) N_c^{-1.20\pm0.13}$ with a correlation coefficient of 0.88 ± 0.09, and covers about 1.5 decade in N_c ($0.05-1\,\mathrm{cm}^{-3}$) and F_v (0.4–0.01). We compare this result with earlier determinations and discuss its meaning for the density structure in Sect. 5.3.

As $F_v(N_c)$ is well defined, we looked for variations with longitude, distance along the plane and height above the plane that may indicate variations in structure in the DIG. We only found a dependence on height: at $|z| < 0.3$ kpc the relationship is considerably steeper and the filling factor for $N_c = 1\,\mathrm{cm}^{-3}$ considerably smaller than at $|z| > 0.3$ kpc (see Fig. 7 and Table 3). The two lines cover nearly the same range in N_c and cross near $N_c = 0.15\,\mathrm{cm}^{-3}$, but at $|z| > 0.3$ kpc the spread in the data is larger than at lower $|z|$. On examination of the much larger sample of BMM, it appears to show the same trend (see Table 3). The large number of pulsars even permits a division of the lower $|z|$–interval yielding exponents of -1.6 ± 0.2 for $|z| < 0.2$ kpc and -1.1 ± 0.1 for $0.2 < |z| < 0.3$ kpc. It seems that in the

Table 3. $|z|$-dependence of the relation $F_v(N_c) = aN_c^b$.

Sample	$\|z\|$ [kpc]	a	b	N	Corr. coeff.	Student t^1
This	0.0–0.3	0.0070 ± 0.0018	-1.55 ± 0.15	15	0.94 ± 0.09	10.2
work	0.3–2.0	0.021 ± 0.006	-0.80 ± 0.17	19	0.80 ± 0.14	5.6
BMM	0.0–0.2	0.0078 ± 0.0020	-1.62 ± 0.16	11	0.97 ± 0.08	12.7
	0.2–0.3	0.0183 ± 0.0037	-1.11 ± 0.12	24	0.91 ± 0.09	10.1
	0.0–0.3	0.0137 ± 0.0023	-1.29 ± 0.10	35	0.92 ± 0.07	13.9
	0.3–2.0	0.0187 ± 0.0014	-1.04 ± 0.03	122	0.95 ± 0.03	31.9

1) Student test: for a sample of $N \geq 11$ pulsars the correlation is significant at the 3σ level if $t > 4.0$.

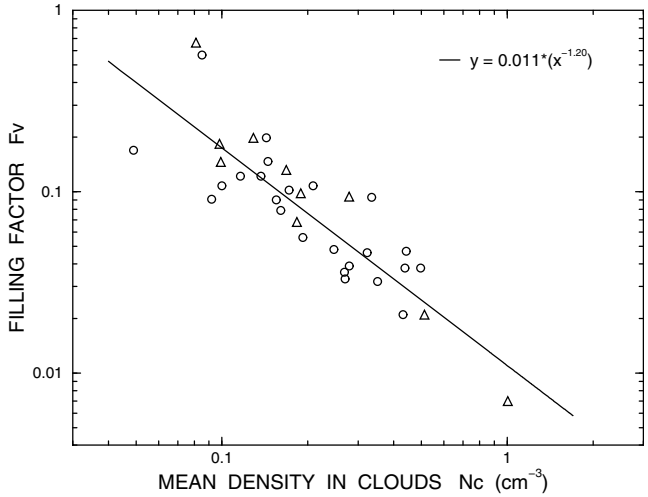

Fig. 6. Dependence of the average volume filling factor, F_v, on the mean density in clouds, N_c, for the sample of 34 pulsars in the solar neighbourhood. Circles: pulsars with $\Delta D/D < 0.2$; triangles: pulsars with $0.2 < \Delta D/D < 0.5$. The full line shows the powerlaw fit given in Table 2.

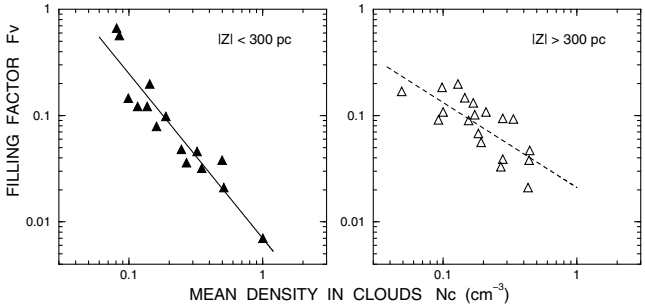

Fig. 7. Dependence of the relation $F_v(N_c)$ on distance to the Galactic plane $|z|$. *Left*: $|z| < 0.3$ kpc; *right*: $|z| > 0.3$ kpc. The lines are powerlaw fits given in Table 3.

thin Galactic disc F_v depends more strongly on N_c than above $|z| = 0.2$ kpc, with an exponent significantly smaller than -1. This indicates that the structure of the DIG in the thin disc differs from that away from the plane. This may not be surprising. In the thin disc the activities of stellar winds, classical H II regions and supernova remnants largely determine the structure of the DIG. They may change or destroy the structure of the turbulence that is typical of more quiet regions away from the Galactic plane. Interestingly, Cordes & Lazio (2002) derived a higher fluctuation factor for the thin disc than for the thick disc in their model of the electron density distribution. There is also evidence from measurements of interstellar scintillation that different types of turbulent spectra exist in different regions of the Galaxy (Shishov et al. 2003).

5. Discussion

5.1. Comparison with BMM 2006

It is interesting to compare our results with those of BMM who took the distances to the pulsars from the NE2001 model of Cordes & Lazio (2002) and used an average correction for the absorption of the Hα emission that only depends on latitude. Applying their method to our sample, we recalculated the main relationships using a scale height of 0.47 kpc to correct for Hα emission from behind the pulsar. Table 4 shows that the resulting relations are nearly identical to those derived in Sect. 4, but with larger errors. This means that the less accurate distances and absorption corrections used by BMM have *not* influenced their statistical results. Therefore, we may compare results from our small sample with those from the much larger sample analysed by BMM with confidence.

A striking difference between the two samples is the behaviour of $F_v(z)$. Where BMM found a significant increase of the filling factor to about 0.2 towards $|z| = 1$ kpc, $F_v(z)$ derived from our sample remains constant within the errors at a value of about 0.08. This difference must be due to the different locations in the Galaxy of the pulsars in the two samples. For example, 17 out of the 34 pulsars (50%) in our sample are within 1 kpc from the Sun, whereas only 44 out of 157 pulsars (28%) of the BMM sample are within this distance. Since the ISM is a highly variable medium, differences between samples are to be expected. Hydromagnetic simulations of the evolution of the ISM by de Avillez & Breitschwerdt (2005) may illustrate this point. Their Fig. 2a shows the density variation in a cut of 1 kpc along and 10 kpc perpendicular to the Galactic plane. Although the filling fraction of the DIG generally increases with height, there are also regions where it remains constant or even decreases away from the plane.

5.2. Extent of ionized regions

The total pathlength through ionized regions perpendicular to the Galactic plane increases nearly linearly from about 7 pc towards $|z| = 100$ pc to about 40 pc towards $|z| = 500$ pc and about 80 pc towards $|z| = 1$ kpc (Fig. 5).

In the ISM dense regions are usually smaller than less dense regions, which also applies to the DIG (see Fig. 8). Although the distribution of $L_e \sin|b|$ with N_c shows considerable spread, it is well fitted by a power law (see Table 2). Regions of density $N_c = 1$ cm^{-3} together occupy about 2 pc in the $|z|$-direction and those of $N_c = 0.05$ cm^{-3} about 300 pc.

Table 4. Comparison with BMM for our sample of 34 pulsars.

Relation	Our data		BMM	
	a	b	a	b
$\langle n_e^2 \rangle = a\, e^{-\lvert z\rvert/b}$	0.0045 ± 0.0007	$1.4^{+0.6}_{-0.3}$	0.0053 ± 0.0011	$1.4^{+1.5}_{-0.5}$
$N_c(z) = a\, e^{-\lvert z\rvert/b}$	0.24 ± 0.04	$2.6^{+4.1}_{1.0}$	0.26 ± 0.06	2^{+10}_{-1}
$F_v(z) = a\, e^{\lvert z\rvert/b}$	0.077 ± 0.018	[23][1]	0.077 ± 0.023	[5][1]
$F_v(N_c) = a\, N_c^b$	0.011 ± 0.003	-1.20 ± 0.13	0.014 ± 0.003	-1.18 ± 0.11

1) Undetermined: $1/b$ smaller than errors.

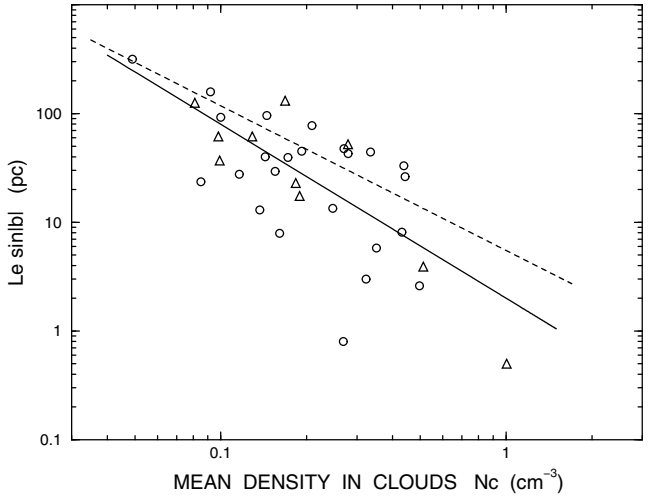

Fig. 8. Dependence of the total pathlength through ionized regions perpendicular to the Galactic plane, $L_e \sin|b|$, on the mean density in clouds, N_c. Circles: pulsars with $\Delta D/D < 0.2$; triangles: pulsars with $0.2 < \Delta D/D < 0.5$. Full line: powerlaw fit given in Table 2; dashed line: powerlaw fit to the sample of 157 pulsars of BMM, $L_e \sin|b|(N_c) = (5.5 \pm 0.8) N_c^{-1.32\pm0.07}$.

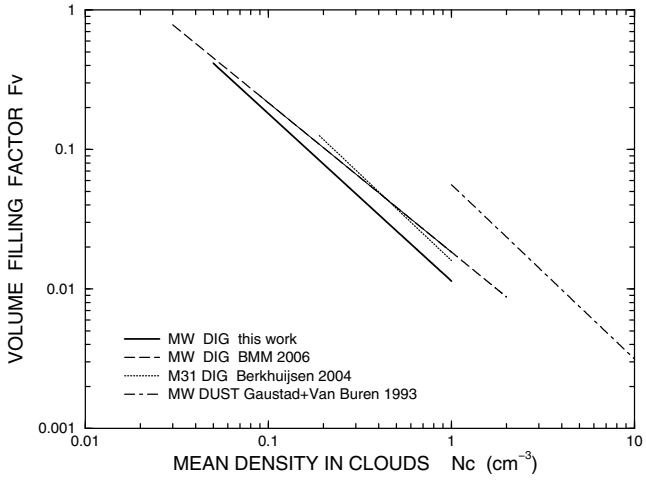

Fig. 9. Dependence of the volume filling factor, F_v, on mean density in clouds, N_c, as derived by different authors. Full line: this work; dashed line: dependence for the DIG within about 3 kpc from the Sun (BMM); dotted line: dependence for the DIG in the bright emission ring in M31 (Berkhuijsen 2004); dash-dot line: dependence for clouds of diffuse dust within 400 pc from the Sun (Gaustad & Van Buren 1993). The parameters of the lines are given in Table 5.

We calculated the same relationship for the BMM sample which gives a somewhat larger extent for the higher densities (see Fig. 8). This power law is close to the one indicated by the distribution of 192 pulsars presented by Hill et al. (2007). However, these authors did not apply any correction to the observed emission measures, which leads to a flattening of the distribution and a shift to higher values of N_c for the same pathlength (see Fig. 5 in BMM).

5.3. The F_v–N_c relation and density structure

of our small sample of pulsars, the nearly inverse correlation between F_v and N_c shown in Fig. 6 is very tight, reaching a correlation coefficient of 0.88 ± 0.09 (see Table 2). It does not change with distance along the plane and, as BMM explained, is insensitive to errors in emission measure. The near constancy of $\langle n_e \rangle = F_v N_c$ along the line of sight (see $D - \langle n_e \rangle$ fit in Table 2), first noted by Weisberg et al. (1980), was an early indication of an inverse relationship between F_v and N_c.

We first compare our F_v–N_c relation with earlier determinations available in the literature, and then discuss what it tells us about the density structure in the DIG.

5.3.1. Comparison with other data

Figure 9 and Table 5 show our F_v–N_c relation together with earlier determinations. For the same mean density in clouds, we find somewhat smaller filling factors than BMM which agree with the lower points in their distribution. The smaller errors in the BMM relation are not only due to the larger sample, but also to the smooth distribution of $\langle n_e \rangle = DM/D$ of the electron density model of Cordes & Lazio (2002) used by BMM. Berkhuijsen (2004) obtained the F_v–N_c relation for the DIG in the galaxy M 31 from a comparison of rotation measures of the polarized continuum emission (giving $\langle n_e \rangle$ with magnetic field strengths of Fletcher et al. 2004) and thermal radio emission (giving $\langle n_e^2 \rangle$). These data refer to the DIG in the bright emission ring in M 31. The good agreement between the M 31 and the MW results suggests that the inverse correlation between F_v and N_c is generally valid in the DIG in galaxies.

Roshi & Anantharamaiah (2001) observed radio recombination lines from the inner Galaxy at low latitudes. They derived filling factors of ≤ 0.01 for extended regions of diffuse ionized gas with densities of 1–10 cm^{-3}, which agree well with the extension of the curves for the DIG in Fig. 9.

Thus the inverse correlation between F_v and N_c at least holds for the density range 0.03–10 cm^{-3}. Cordes et al. (1985) estimated a filling factor of $10^{-4.0\pm0.3}$ for clumps of about 1 pc size causing scattering of pulsar signals. Our data predict this filling factor for clumps of density $N_c = 50$ cm^{-3} and size $L_e/m = 0.9$ pc, where m is the number of clumps on the line of sight. The relation of BMM gives clumps of $N_c = 100$ cm^{-3} for the same filling factor and sizes. So these clump properties also seem to follow the F_v–N_c relations derived for the DIG.

Table 5. Comparison of $F_v - N_c$ relations $F_v(N_c) = a\,N_c^b$.

Sample	a	b	Range N_c [$\mathrm{cm^{-3}}$]	Range F_v	Ref.
DIG					
MW $N = 34$	0.0114 ± 0.0025	-1.20 ± 0.13	0.05–1	0.4–0.011	1
MW $N = 157$	0.0184 ± 0.0011	-1.07 ± 0.03	0.03–2	0.8–0.009	2
M31	0.016 ± 0.004	-1.24 ± 0.30	0.19–1	0.13–0.016	3
DIFFUSE DUST					
$D < 400$ pc	0.056 ± 0.020	-1.25 ± 0.40	1–10	0.06–0.003	4

References. (1) This work; (2) Berkhuijsen et al. (2006); (3) Berkhuijsen (2004); (4) Gaustad & Van Buren (1993).

Furthermore, Gaustad & Van Buren (1993) obtained a similar relationship for clouds of diffuse dust within 400 pc from the Sun, with mean densities of 1–10 $\mathrm{cm^{-3}}$. Figure 9 shows that these clouds have about 3 times higher filling factors than ionized clouds of the same mean density. Interestingly, their data agree very well with those of Pynzar (1993; also shown in Berkhuijsen 1998) derived from recombination lines.

5.3.2. Density structure of the DIG

The general validity of the inverse F_v–N_c relation indicates that it describes a basic property of the DIG, possibly even of the entire ISM (Berkhuijsen 1999). At least two mechanisms could be responsible: thermal pressure equilibrium and turbulence causing a fractal density structure.

Thermal pressure equilibrium leads to an inverse F_v–N_c relation if it is widespread, but it seems only locally valid. In the MW large fractions of gas are observed in unstable regimes and have also been found in simulations of a turbulent ISM. Thermal pressure equilibrium of clouds appears to be of minor importance in the presence of turbulence (see Elmegreen & Scalo 2004, and references therein).

Elmegreen (1998, 1999) discussed the properties of diffuse ionized gas in a pervasive fractal ISM. One of these properties is an inverse correlation between volume filling factor and gas density, which is expected on theoretical grounds (Fleck 1996) as well as from simulations (Elmegreen 1997; Kowal & Lazarian 2007). As this leads to a constant average density along the line of sight, the observed near constancy of $\langle n_e \rangle$ with N_c and F_v inversely varying over 1.5 decade may indicate that the density distribution of the DIG is fractal. However, the near constancy of $\langle n_e \rangle$ alone should only be regarded as a first indication, because the fits in Table 2 show that the statistical significance of the near constancy of $\langle n_e \rangle$ is much lower than that of the nearly inverse F_v–N_c relation.

The fractal medium is characterized by filamentary, clumpy structures that tend to cluster together, with holes inside and large voids between them. The filling factor along the line of sight is determined by the outer regions of the filaments, i.e. by the largest scales, because the small, dense clumps in the inner parts hardly contribute. The voids occupy more space than the filaments, thus the filling factor of the filaments is small. The values of $F_v \simeq 0.1$ (Sect. 4.1) and $F_v \simeq 0.2$ (BMM) obtained when looking perpendicular to the Galactic plane towards $|z| = 1$ kpc are consistent with this picture.

The tendency of filaments to cluster into larger complexes reduces the number of fractal clouds, N_f, along the line of sight. Elmegreen (1998) estimated $N_f = 3$/kpc locally. For $F_v = 0.1$ the total pathlength through the ionized regions is 100 pc/kpc, giving a line of sight through one fractal complex of about 30 pc and a mean density N_c of 0.15 $\mathrm{cm^{-3}}$ (from Fig. 6). Using the results of BMM gives $F_v = 0.2$, a fractal complex of about 70 pc along the line of sight and $N_c = 0.10\,\mathrm{cm^{-3}}$. Interestingly, these pathlengths are in the range of 10–100 pc that Ohno & Shibata (1993) estimated for the cells of ionized gas causing *DM* and rotation measure *RM* towards pairs of pulsars close on the sky.

According to Elmegreen (1998), a pervasive fractal structure only develops in regions outside the influence of SN shells, sites of star formation, chimneys etc. that are concentrated near the Galactic plane. This may explain our result of Sect. 4.2 that the exponent of the F_v–N_c relation is significantly smaller in the thin disc ($|z| < 300$ pc) than further from the plane where it is close to -1 (see Table 3 and Fig. 7).

We conclude that our results on the mean electron densities and volume filling factors of the DIG outside the thin disc are consistent with a fractal ionized medium caused by turbulence, while the structure in the thin disc is dominated by the effects of SN shocks, stellar winds, star formation and other forces. The difference in density structure between these two regimes could be further analysed when more pulsars with measured distance become available.

Recently, further observational evidence for a turbulent structure of the DIG and of the diffuse atomic gas has been presented. Hill et al. (2008) found that the probability distribution function (PDF) of the emission measures observed perpendicular to the Galactic plane at $|b| > 10°$ is lognormal, as is expected for a turbulent medium from MHD simulations of the ISM (Elmegreen & Scalo 2004). Furthermore, Berkhuijsen & Fletcher (2008) showed that the PDFs of the quantities $\langle n_e \rangle$, $\langle n_e^2 \rangle$, N_c and F_v derived above as well as that of the mean H I density along the line of sight towards stars, $\langle n_{HI} \rangle$, are lognormal, consistent with a turbulent origin of density structure in the diffuse gas.

6. Summary

We have used pulsar dispersion measures (Manchester et al. 2005) and extinction-corrected emission measures (Finkbeiner 2003; Dickinson et al. 2003) towards 38 pulsars with known distances for a statistical study of several parameters of the diffuse ionized gas (DIG) in the Solar neighbourhood. The emission measures were also corrected for contributions from beyond the pulsar distance. To avoid regions with strong absorption (>1 mag) and contributions from H II regions most pulsars in the sample are at Galactic latitudes $|b| > 5°$. The statistical results are collected in Tables 2 and 3.

Our main conclusions are:

1. From the scaling of dispersion measures with distance perpendicular to the Galactic plane, we find a scale height of the ionized layer of 0.93 ± 0.13 kpc and an electron density

at the midplane of $0.023 \pm 0.004\,\mathrm{cm}^{-3}$, in good agreement with earlier determinations.

2. The dispersion measure DM and the corrected emission measure EM_p are well correlated, indicating that they probe the same ionized regions. We may then combine them to derive the average densities along the line of sight, $\langle n_\mathrm{e}\rangle$ and $\langle n_\mathrm{e}^2\rangle$, the mean electron density in clouds in the line of sight, N_c, the volume filling factor of these clouds, F_v, and the total pathlength through the ionized regions, L_e.
3. The total extent of the ionized regions perpendicular to the Galactic plane increases linearly reaching about 80 pc towards $|z| = 1$ kpc.
4. The filling factor F_v remains essentially constant with $|z|$ at a mean value of 0.08 ± 0.02. Whether $F_\mathrm{v}(z)$ is constant or systematically increases with $|z|$ depends on the regions in the Galaxy probed by the pulsar sample.
5. The average electron density $\langle n_\mathrm{e}\rangle$ is about constant with a spread of a factor $\lesssim$2 about the mean value of $0.018 \pm 0.002\,\mathrm{cm}^{-3}$. Since $\langle n_\mathrm{e}\rangle = F_\mathrm{v} N_\mathrm{c}$, an inverse relationship between F_v and N_c is expected.
6. We derived the relation $F_\mathrm{v}(N_\mathrm{c}) = (0.011 \pm 0.003) N_\mathrm{c}^{-1.20\pm0.13}$, which covers about 1.5 decade in N_c ($0.05 - 1\,\mathrm{cm}^{-3}$) and F_v ($0.4 - 0.01$) (see Fig. 6). This is in good agreement with earlier determinations of the F_v–N_c relations for the DIG (see Fig. 9).
7. Near the Galactic plane the dependence of F_v on N_c is significantly stronger than away from the plane. This indicates that the thin disc has a different turbulent structure than regions away from the plane.
8. The inverse relationship between F_v and N_c, and hence also the near constancy of $\langle n_\mathrm{e}\rangle$, are consistent with a fractal density distribution in the DIG caused by turbulence which dominates the structure outside the thin disc.

Acknowledgements. We thank Dr. Rainer Beck for careful reading of the manuscript and useful suggestions, and the referee for helpful comments leading to improvements in the manuscript.

References

Bailes, M., Manchester, R. N., Kesteven, M. J., et al. 1990, Nature, 343, 240
Bennett, C. L., Hill, R. S., Hinshaw, G., et al. 2003, ApJS, 148, 97
Berkhuijsen, E. M. 1998, in The Local Bubble and Beyond, ed. D. Breitschwerdt, M. J. Freyberg, & J. Trümper, Lect. Notes Phys., 506, 301
Berkhuijsen, E. M. 1999, in Plasma Turbulence and Energetic Particles in Astrophysics, ed. M. Ostrowski, & R. Schlickeiser (Krakow: Astron. Obs. Jagiellonian Univ.), 61
Berkhuijsen, E. M. 2004, Ap&SS, 289, 207
Berkhuijsen, E. M., & Fletcher, A. 2008, MNRAS Lett., in press [arXiv:0806.4316V1]
Berkhuijsen, E. M., Mitra, D., & Müller, P. 2006, AN, 327, 82 (=BMM)
Bhattacharia, D., & Verbunt, F. 1991, A&A, 242, 128
Brisken, W. F., Benson, J. M., Goss, W. M., et al. 2002, ApJ, 571, 906
Brisken, W. F., Thorsett, S. E., Golden, A., et al. 2003, ApJ, 593, L89
Chatterjee, S., Cordes, J. M., Lazio, T. J. W., et al. 2001, ApJ, 550, 287
Chatterjee, S., Vlemmings, W. H. T., Brisken, T. J. W., et al. 2005, ApJ, 630, L61
Cordes, J. M., & Lazio, T. W. J. 2002 [arXiv:astro-ph/0207156]
Cordes, J. M., & Lazio, T. W. J. 2003 [arXiv:astro-ph/0301598]
Cordes, J. M., Weisberg, J. M., & Boriakoff, W. 1985, ApJ, 288, 221
de Avillez, M. A., & Breitschwerdt, D. 2005, A&A, 436, 585
Dickinson, C., Davies, R. D., & Davis, R. J. 2003, MNRAS, 341, 369
Diplas, A., & Savage, B. D. 1994, ApJ, 427, 274
Elmegreen, B. G. 1997, ApJ, 477, 196
Elmegreen, B. G. 1998, PASAu, 15, 74
Elmegreen, B. G. 1999, in The Physics and Chemistry of the Interstellar Medium, 3rd Cologne-Zermatt Symposium, ed. V. Ossenkopf, J. Stutzki, & G. Winnewisser (Aachen: Shaker), 77
Elmegreen, B. G., & Scalo, J. 2004, ARA&A, 42, 211
Finkbeiner, D. P. 2003, ApJ, 146, 407
Fleck, R. C. 1996, ApJ, 458, 739
Fletcher, A., Berkhuijsen, E. M., Beck, R., & Shukurov, A. 2004, A&A, 414, 53
Gaustad, J. E., & Van Buren, D. 1993, PASP, 105, 1127
Gomez, G. C., Benjamin, R. A., & Cox, D. P. 2001, AJ, 122, 908
Gwinn, C. R., Taylor, J. H., Weisberg, J. M., et al. 1986, AJ, 91, 3383
Haffner, L. M., Reynolds, R. J., & Tufte, S. L. 1998, ApJ, 501, L83
Haffner, L. M., Reynolds, R. J., Madsen, G. J., et al. 2003, ApJS, 149, 405
Heitsch, F., & Richtler, T. 1999, A&A, 347, 455
Hill, A. S., Reynolds, R. J., Benjamin, R. A., & Haffner, L. M. 2007, ASP Conf. Ser., 365, 250
Hill, A. S., Benjamin, R. A., Kowal, G., et al. 2008, ApJ, in press [arXiv:0805.0155V2]
Hinshaw, G., Nolta, M. R., Bennett, R., et al. 2007, ApJS, 170, 288
Hobbs, G. B., & Manchester, R. N. 2003, http://www.atnf.csiro.au/research/pulsar/psrcat
Hobbs, G., Lorimer, D. R., Lyne, A. G., & Kramer, M. 2005, MNRAS, 360, 974
Hotan, A. W., Bailes, M., Ord, S. M., et al. 2006, MNRAS, 369, 1502
Kowal, G., & Lazarian, A. 2007, ApJ, 666, L69
Kulkarni, S. R., & Heiles, C. 1988, in Galactic and Extragalactic Radio Astronomy, ed. G.A. Verschuur, & K.I. Kellermann (New York: Springer), 95
Löhmer, O., Kramer, M., Driebe, T., et al. 2004, A&A, 426, 631
Lommen, A. N., Kipphorn, R. A., Nice, D. J., et al. 2006, ApJ, 642, 1012
Lorimer, D. R. 2004, in Young Neutron Stars and Their Environments, ed. F. Camilo, & B. M. Gaensler (San Francisco: ASP), IAU Symp., 218, 105
Madsen, G. J., Reynolds, R. J., & Haffner, L. M. 2006, ApJ, 652, 401
Manchester, R. N., Hobbs, G. B., Teoh, A., & Hobbs, M. 2005, AJ, 129, 1993
Nordgren, T. E., Cordes, J. M., & Terzian, Y. 1992, AJ, 104, 1465
Ohno, H., & Shibata, S. 1993, MNRAS, 262, 953
Pynzar, A. V. 1993, ARep, 37, 245
Reynolds, R. J. 1991a, ApJ, 372, L17
Reynolds, R. J. 1991b, in The Interstellar Disk-Halo Connection in Galaxies, ed. H. Bloemen (Dordrecht: Kluwer), IAU Symp., 144, 67
Reynolds, R. J. 1997, in The Physics of Galactic Haloes, ed. H. Lesch, R. J. Dettmar, U. Mebold, & R. Schlickeiser (Berlin: Akademie), 57
Roshi, D. A., & Anantharamaiah, K. R. 2001, ApJ, 557, 226
Shishov, V. I., Smirnova, T. V., Sieber, W., et al. 2003, A&A, 404, 557
Stairs, I. H., Arzoumanian, Z., Camilo, F., et al. 1998, ApJ, 505, 352
Weisberg, J. M., Rankin, J., & Boriakoff, V. 1980, A&A, 88, 84
Yusifov, I., & Küçük, I. 2004, A&A, 422, 545